Published in final edited form as:
J Immunol. 2012 March 1; 188(5): 2093–2101. doi:10.4049/jimmunol.1101118.

Adjuvant immunotherapy of Experimental Autoimmune Encephalomyelitis: Immature Myeloid Cells Expressing CXCL10 and CXCL16 attract CXCR3^{+}CXCR6^{+} and myelin-specific T cells to the draining lymph nodes rather than the CNS [1,,2]

Richard A. O'Connor[†,2], **Xujian Li**[*,2], **Seth Blumerman**[‡], **Stephen M. Anderton**[†], **Randolph J. Noelle**[§,¶], and **Dyana K. Dalton**[§,3]

[†]Medical Research Council/University of Edinburgh Centre for Inflammation Research, Centre for Multiple Sclerosis Research, Queen's Medical Research Institute, 47 Little France Crescent, Edinburgh EH16 4TJ. UK

[*]Toronto General Research Institute, Room 2-807, Toronto Medical Discovery Tower, 101 College St., Toronto, ON M5G 1L7, Canada

[‡]Department of Biological Sciences, University of Delaware, Newark, DE 19716

[§]Department of Microbiology and Immunology, Dartmouth Medical School and The Norris Cotton Cancer Center, 1 Medical Center Drive, Lebanon, NH 03756, USA

[¶]Department of Nephrology and Transplantation, MRC Centre for Transplantation, King's College London, 5th Floor Tower Wing, Guy's Hospital, London, SE1 9RT, UK

Abstract

CFA is a strong adjuvant capable of stimulating cellular immune responses. Paradoxically, adjuvant immunotherapy by prior exposure to CFA or live mycobacteria suppresses the severity of EAE and spontaneous diabetes in rodents. Here we investigated immune responses during adjuvant immunotherapy of experimental autoimmune encephalomyelitis (EAE). Induction of EAE in CFA-pretreated mice resulted in a rapid influx into the draining lymph nodes (dLNs) of large numbers of CD11b^{+}Gr-1^{+} myeloid cells, consisting of immature cells with ring-shaped nuclei, macrophages, and neutrophils. Concurrently, a population of mycobacteria-specific IFN-γ-producing T cells appeared in the dLNs. Immature myeloid cells in dLNs expressed the chemokines CXCL10 and CXCL16 in an IFN-γ-dependent manner. Subsequently, CD4^{+} T cells co-expressing the cognate chemokine receptors, CXCR3 and CXCR6, and myelin oligodendrocyte glycoprotein (MOG)-specific CD4^{+} T cells accumulated within the chemokine-expressing dLNs, rather than within the CNS. Migration of CD4^{+} T cells toward dLN cells was abolished by depleting the CD11b^{+} cells and was also mediated by the CD11b^{+} cells alone. In addition to altering the distribution of MOG-specific T cells, adjuvant-treatment suppressed development of MOG-specific IL-17. Thus, CFA-adjuvant immunotherapy of EAE requires IFN-γ, which

[1]This work was supported by the following grants: National Institute of Health grants: NS 043355 (DKD) and CA123079 (RJN); and National Multiple Sclerosis Society grants RG 3103 (DKD), RG 3820 (DKD) and FG 1513 (ROC)

[3]Correspondence: Dyana K. Dalton, Dyana.Dalton@Dartmouth.edu (603) 359-0977, Fax. 603-653-9952.
[2]R.O.C. and X.L. co-first authors, contributed equally to this work.

suppresses development of the Th17-response, and diverts autoreactive T cells away from the CNS towards immature myeloid cells expressing CXCL10 and CXCL16 in the lymph nodes.

Introduction

EAE is an organ-specific model of autoimmunity in the CNS and is a widely studied model of the human autoimmune disease multiple sclerosis (MS) (1). EAE is induced by immunizing mice with myelin antigens emulsified in CFA, the latter consisting of killed mycobacteria in mineral oil. Mycobacteria express antigens, TLR agonists, and heat-shock proteins promoting Th1 responses and delayed-type hypersensitivity against injected self-antigens (2). Since CFA is considered to be a strong adjuvant capable of stimulating cellular immune responses, it is paradoxical that prior exposure to CFA suppresses the severity of EAE (3). Similarly, adjuvant immunotherapy with live mycobacterial infection also ameliorates the severity of EAE (4, 5).

Adjuvant immunotherapy is not limited to experimental autoimmune diseases that are induced with CFA. Notably, live mycobacteria and CFA both suppress spontaneous disease in non-obese diabetic (NOD) mice, thus enabling regeneration of pancreatic cells in treated mice (6–11). Adjuvant-mediated suppression of autoimmune disease in rodents can persist as long as a year (12). The success of adjuvant immunotherapy in preclinical models of autoimmune disease has prompted recent clinical trials of adjuvant immunotherapy using live BCG vaccine in humans with autoimmune diabetes (13).

Although both CFA and live mycobacteria suppress EAE and autoimmune diabetes in preclinical models, their mechanisms of immune suppression may not be identical. CFA-treatment has been reported to promote T cell dormancy, as demonstrated by adjuvant-treated mice harboring autoreactive T cells capable of transferring autoimmune disease to recipient mice (14). Alternatively, CFA-treatment was reported to eliminate a population of TNF-α-susceptible cells, suggesting that CFA-treatment resulted in deletion of autoreactive cells rather than dormancy (9). When considering therapies to halt autoimmune destruction, treatments promoting deletion of autoreactive T cells and treatments promoting dormancy of autoreactive T cells may have different outcomes. For this reason, it is important to understand mechanisms of adjuvant immunotherapy by live and killed bacteria.

We have previously demonstrated that an ongoing infection of mice with live mycobacteria suppressed EAE by promoting IFN-γ-dependent apoptosis of MOG-specific $CD4^+$ T cells in a bystander fashion (4). Here we investigated the mechanism by which killed mycobacteria in CFA attenuates EAE. Our data indicate that CFA does not result in enhanced apoptosis of CNS-infiltrating $CD4^+$ T cells. Instead, we provide evidence for a novel mechanism for CFA-adjuvant immunotherapy that is, in part, dependent on IFN-γ. Suppression of EAE by CFA is associated with a rapid simultaneous influx of immature myeloid cells and IFN-γ-producing T cells into the lymph nodes draining the EAE induction site. The myeloid cells in WT, but not IFN-$\gamma^{-/-}$ mice, expressed Th1 cell-attracting chemokines CXCL10 and CXCL16. Subsequently, a large population of $CD4^+$ T cells expressing both CXCR3 and CXCR6 as well as MOG-specific T cells accumulated within the chemokine-expressing lymph nodes, instead of within the CNS. Also, in WT mice,

development of the MOG-specific IL-17 response was suppressed by CFA-pretreatment; in contrast adjuvant treatment failed to suppress IL-17 production in IFN-$\gamma^{-/-}$ mice. IFN-$\gamma^{-/-}$ mice were not protected from clinical EAE by CFA-adjuvant therapy. Thus, CFA-adjuvant immunotherapy of EAE requires IFN-γ, which suppresses development of the Th17-response, and diverts autoreactive T cells away from the CNS towards immature myeloid cells expressing CXCL10 and CXCL16 in the lymph nodes.

Materials and Methods

Mice

Female mice were used in all experiments. Breeding stocks for IFN-$\gamma^{-/-}$ C57BL/6 background and C57BL/6 mice were obtained from the Jackson Laboratories (Bar Harbor, Maine). All investigations involving mice were carried out in accordance with standards and protocols approved by Institutional Animal Care and Use Committee (IACUC) at Trudeau Institute, University of Edinburgh, Toronto General Research Institute, and Dartmouth Medical School.

Adjuvant treatment

Mice were immunized with CFA on the left flank with 50 μl of a 1:1 CFA/PBS emulsion. CFA contained 4 mg/ml of killed *Mycobacterium tuberculosis* (H37Ra) and 0.4 mg/ml *Mycobacterium butyricum* (Difco).

Induction and clinical scoring of EAE

Naïve and adjuvant-treated mice were immunized on the right flank with 100 μg of myelin-oligodendrocyte glycoprotein peptide, amino acid residues 35–55 (MOG) (from American Peptide, Sunnyvale, CA) emulsified in CFA (50μl volume). The dramatic changes in the right inguinal dLN in response to EAE induction were evident in adjuvant-treated mice, but not naïve mice that were induced to develop EAE. At the time of EAE induction and 48 hours later, mice were injected intraperitoneally with 200 ng of pertussis toxin (Sigma). Mice were observed daily for disease symptoms and assigned a score of 0–5 as follows: 0, no sign of paralysis; 1, weak tail; 2, paralyzed tail; 3, paralyzed tail and weakness of hind limbs (wobbly gait); 4, completely paralyzed hind limbs; 5, moribund. Scores were assigned using 0.5 unit increments when symptoms were intermediate.

Isolation of mononuclear cells—Inguinal lymph nodes were removed and single cell suspensions prepared by gently pressing and washing cells through a 70 μm mesh screen. Mononuclear cells in the CNS were isolated using Percoll gradient centrifugation as described (15). Briefly, peripheral blood was removed from the CNS by perfusion and then the CNS was removed and dissociated by washing through a 100 micron mesh. The cells were then centrifuged through a 30:37:70% discontinuous Percoll gradient. Mononuclear cells at the 37%:70% Percoll interface were collected and stained for phenotypic analysis.

ELISPOT assay—The frequency of IFN-γ-producing cells in the CNS and dLNs was determined using an IFN-γ- specific ELISPOT kit (BD Biosciences) according to the manufacturer's instructions. CNS mononuclear cells (1×10^4 to 2.5×10^5 cells/well) and

lymph node cells were plated at various densities in an ELISPOT plate coated with rat anti-mouse IFN-γ capture antibody in the presence or absence of 10 μg/ml (MOG). In Fig 2D, 10 μg/ml final concentration of Mycobacterium tuberculosis (desiccated, sonicated in PBS) was used to stimulate IFN-γ production in the ELISPOT assay. Cells were cultured overnight, lysed, and IFN-γ production detected using a biotin-conjugated rat anti-mouse IFN-γ detection antibody. Avidin-horseradish peroxidase was then added, and spots were developed with 3-amino-9-ethylcarbamazole (AEC). Specific IFN-γ production was calculated by subtracting the background (medium-only) from specific antigen-stimulated spots.

Analysis of cytokine production following adjuvant pretreatment

Wild type and IFN-$\gamma^{-/-}$ mice were adjuvant pre-treated with a subcutaneous injection of 50 μl of CFA on the left flank, control mice were left untreated (n=6 per group). 21 days later mice were immunized with 100 μg MOG in CFA on the right flank. Seven days post MOG-immunization, mice were sacrificed and draining lymph node cells and splenocytes (both at 0.5×10^6 / ml) were re-stimulated with graded doses of MOG. Supernatants were collected after 72 hrs culture for analysis of cytokine production by ELISA (IL-17 / IFN-γ) or Flowcytomix cytokine bead array (GM-CSF) according to the manufacturer's instructions (eBioscience, San Diego).

FACS analysis of cell subsets—Single cell suspensions in a defined volume were counted on a hemacytometer using trypan blue exclusion of dead cells to determine total live cell numbers. The absolute number of cells was calculated for each sample by applying the percentage of each subset to the total live cells in lymph nodes or CNS. CNS-infiltrating cells and peripheral lymphocytes were prepared for FACS by staining with anti-CD4 PE (L3T4), CD11b APC / PE (M1/70), Gr-1 (IA8), CD45 APC (30-F11), anti-CXCR3 (CXCR3-173), rat anti-mouse CXCR6 (clone 221002), goat anti-rat-PE to detect cell surface expression of CXCR6 (all antibodies were from eBiosciences or BD Biosciences). As the unconjugated CXCR6 primary antibody was detected by a PE-conjugated anti-rat secondary antibody, the two-step CXCR6 staining was done, cells were washed, then other surface antigens were detected with their primary antibodies. Cells were gated based on forward and side scatter and PI^+ or $7AAD^+$ (dead) cells excluded from analysis.

Chemokine microarray—WT and IFN-$\gamma^{-/-}$ mice were treated with CFA on the left flank and rested for 3 weeks. EAE then was induced by immunizing mice with MOG-peptide in CFA, on the right flank, according to the above protocol. 24 hours later the right lymph nodes were isolated and pooled from five mice per group. The $CD11b^+Gr\text{-}1^+$ cells were FACS-sorted from WT and IFN-$\gamma^{-/-}$ lymph nodes and RNA was prepared from the cells with Trizol (Invitrogen). An initial survey of chemokine and receptor transcripts was done by hybridizing equal amounts of RNA (2 μg per sample) to chemokine microarrays: GEArray Q Series Mouse Chemokines and Receptors Gene Array (OMM-022, Superarray). Arrays were processed, developed, and analyzed according to the manufacturer's instructions.

Chemotaxis assay

The lower wells of transwell plates were seeded with 2×10^6 cells in all conditions. As indicated Fig. 4A, we used whole dLNs, lymph-node cells from EAE-only or adjuvant-EAE mice. Magnetic beads (Miltenyi) were used to deplete $CD11b^+$ cells and to enrich $CD11b^+$ cells from whole dLNs. $CD4^+$ T cells, MACS-isolated from the dLNs of adjuvant-EAE mice, were stained with FITC after isolation. An input number of 2×10^5 $CD4^+$FITC-labeled T cells were added to the upper wells. The cells were cultured for 2 hr in a CO_2 incubator at 37°C. After removing top well inserts, the cells in the lower wells were collected, washed, and stained with a fixable viability marker eFluor450 (eBioscience), then adjusted to 0.4 ml for collection on the flow cytometer. CountBright beads (Invitrogen) were used to calculate the absolute numbers of $CD4^+FITC^+$ cells in the lower wells according to manufacturer's instructions. Using absolute counts and known numbers of cells on the top wells, the percentage of input cells that migrated toward the lower wells was calculated.

RT PCR

Inguinal lymph nodes were removed and immediately snap frozen. RNA was prepared using RNeasy kits (Qiagen) according to the manufacturer's instructions. RNA was DNAse treated using a DNA-free kit according to the manufacturer's instructions (Ambion). RNA was reverse transcribed using Superscript II reverse transcriptase, random primers and dNTPs (all Invitrogen). Expression levels in EAE-only samples were compared to those in naïve mice to establish any differences resulting from EAE induction. Likewise, expression levels in adjuvant-EAE mice were compared to naïve and EAE only samples. All PCR reactions were done in duplicate and the mean values of each group were calculated from 3–6 individual animals.

Results

Adjuvant-immunotherapy with CFA attenuated EAE without increasing apoptosis of T cells in the CNS

The adjuvant-treated mice were injected with CFA on the left flank. After resting adjuvant-treated mice for three weeks, EAE was induced in adjuvant-treated and naïve mice by giving a single s.c.injection of MOG peptide emulsified in CFA in the right flank. Induction of EAE in adjuvant-treated mice constituted a secondary challenge with CFA, which was manifested within 24 hours as a striking enlargement of the right inguinal LNs draining the second CFA injection site. Lymph node enlargement was only apparent in adjuvant-treated mice and was confined to the lymph nodes draining the site of MOG/CFA immunization. In the experiments that are detailed below we investigated the cellular and molecular changes in the right dLNs of adjuvant-treated mice with EAE compared with EAE-only mice (Fig 1A).

Treatment of WT mice with CFA three weeks before inducing EAE significantly attenuated the clinical symptoms of disease (Fig. 1B) compared with non-adjuvant-treated mice with EAE. Previously we had shown that mice infected with live mycobacteria (*Mycobacterium bovis*, strain BCG) also exhibited attenuated EAE. Importantly, BCG infection increases the apoptosis of activated bystander T cells, indicating that the viability of autoantigen-reactive

T cells was impaired during BCG-infection (4). To investigate whether CFA also increased apoptosis of CNS-infiltrating $CD4^+$ T cells we measured apoptosis using the Annexin-V assay. Unlike live BCG infection, CFA pretreatment did not induce high levels of apoptosis in CNS-infiltrating $CD4^+$ T cells on day 15 of disease (Fig.1C). Thus, although BCG and CFA both attenuated EAE, only live mycobacteria caused high levels of apoptosis of $CD4^+$ T cells in the CNS.

Adjuvant treated mice responded to EAE induction by rapidly mobilizing immature myeloid cells and mycobacterial Ag-specific IFN-γ^+ T cells to the right lymph nodes

In adjuvant-treated mice enlargement of the right lymph nodes at 24 hours post-EAE induction reflected increased numbers of total cells (8-fold), $CD4^+$ T cells (5-fold) and $CD11b^+Gr\text{-}1^+$ myeloid cells (20-fold) (Figs. 2A, B, and C). We considered that the re-exposure of adjuvant-treated mice to CFA may have recruited mycobacterial Ag-specific effector T cells to the right dLNs. Indeed, an ELISPOT assay showed that adjuvant-treated mice have a high frequency of mycobacteria-specific IFN-γ^+ T cells in the right dLNs within 24 hours of EAE induction (Fig. 2D). As expected, control mice immunized to develop EAE had no detectable mycobacteria-specific T cells in their right lymph draining nodes at the same time point.

In adjuvant-treated mice with EAE, the increased numbers of mycobacteria-reactive IFN-γ^+ cells coincided with accumulation of large numbers of $CD11b^+$ $Gr\text{-}1^+$ myeloid cells in the right dLNs. Such myeloid cells were present at a low frequencies and numbers in dLNs of naïve mice and EAE-only mice at 24 hours after immunization (Figs. 2C and E). FACS-purified myeloid cells from adjuvant-EAE lymph nodes were examined in cytospin preparations. The cells were heterogeneous, with many having ring-shaped nuclei characteristic of immature myeloid-lineage cells as well as some resembling mature granulocytes and macrophages (Fig. 2F). These results indicate that upon EAE induction in adjuvant-treated mice, there is a rapid and coordinated influx of myeloid cells, $CD4^+$ T cells, and mycobacteria-specific IFN-γ^+ cells into the right inguinal lymph nodes draining the site of re-exposure to CFA.

$CD11b^+Gr\text{-}1^+$ cells in the right lymph nodes of adjuvant-treated WT, but not IFN-$\gamma^{-/-}$, mice expressed high levels of IFN-γ-inducible CXCL10 and CXCL16

IFN-γ expressed by T cells in the right dLNs of adjuvant-EAE mice could contribute to adjuvant-mediated protection from EAE. Thus, we tested whether adjuvant could protect IFN-$\gamma^{-/-}$ mice from EAE. Adjuvant-treated IFN-$\gamma^{-/-}$ mice initially developed EAE with slower onset (as reflected by significantly reduced clinical severity on day 14) compared with untreated IFN-$\gamma^{-/-}$ mice. However, by day 21, the disease scores of adjuvant-treated and untreated mice IFN-$\gamma^{-/-}$ mice with EAE were similar Fig. 3A). This contrasted with WT mice in which adjuvant treatment provided significant protection from EAE ($p=0.02$) throughout the monitoring period (compare Fig. 1B to Fig 3A). Severe EAE in adjuvant-treated IFN-$\gamma^{-/-}$ mice demonstrates that IFN-γ contributes to suppression of EAE by adjuvant immunotherapy. The comparative rate of recovery in adjuvant-treated versus untreated IFN-$\gamma^{-/-}$ mice was not assessed for humane reasons because of the severe EAE in IFN-$\gamma^{-/-}$ mice.

$CD4^+$ T cells were present at significantly higher numbers in dLNs of adjuvant-treated mice with EAE (Fig. 2B), raising the possibility of their increased migration to or retention within the dLNs. Our preliminary investigations suggested that myeloid cells in adjuvant-treated mice were a source of chemokines. Moreover, although IFN-$\gamma^{-/-}$ mice were not fully protected by adjuvant-treatment, they also accumulated a large population of $CD11b^+Gr\text{-}1^+$ cells in the right dLN upon EAE induction. Such accumulation is consistent with previous work showing that CFA expands a population of immature myeloid cells, which is restrained by IFN-γ (16). Thus, we FACS-sorted dLN $CD11b^+Gr\text{-}1^+$ cells from adjuvant-treated WT and IFN-$\gamma^{-/-}$ mice with EAE and prepared RNA for analysis of chemokine gene expression. Chemokine microarrays showed that myeloid cells from WT adjuvant-treated mice expressed high levels of the chemokines CXCL10 and CXCL16, both of which can be induced in myeloid cells in response to IFN-γ (17, 18) (Fig 3B). However, CXCL10 and CXCL16 transcripts were completely absent in myeloid cells from adjuvant-treated IFN-$\gamma^{-/-}$ mice (Fig. 3B). These results indicate that in our model, an intact IFN-γ gene is required for expression of CXCL10 and CXCL16 by myeloid cells in the dLNs.

Next, the expression of IFN-γ, CXCL10 and CXCL16 within whole dLN cells was validated using RT PCR (Fig. 3C). Adjuvant-treated mice with EAE expressed over 40-fold higher levels of CXCL10 and 6–8-fold higher levels of CXCL16 transcripts, relative to controls on day 1, but the transcripts returned to baseline levels on day 7.

$CD11b^+$ myeloid cells from the dLNs of adjuvant-treated mice induce the migration of $CD4^+$ T cells

We next tested whether dLNs from adjuvant-treated mice were able to induce migration of $CD4^+$ T cells. In a transwell chemotaxis assay, dLN cells from adjuvant-treated mice with EAE, but not dLN cells from EAE-only mice, induced significant migration of activated $CD4^+$ T cells (Fig. 4A). Moreover, migration of $CD4^+$ T cells toward the adjuvant-treated dLN cells was completely abolished by depletion of the $CD11b^+$ cells. Further, pure populations of $CD11b^+$ cells isolated from adjuvant-treated dLNs induced significant $CD4^+$ T cell migration towards the myeloid cells. These data indicate that the $CD11b^+$ myeloid cells, demonstrated to produce CXCL10 and CXCL16 transcripts (Fig 3B), constitute the major population of dLN cells in adjuvant- EAE mice that induce chemotaxis of $CD4^+$ T cells.

We also investigated the in vivo kinetics of $CD4^+$ T cell migration into chemokine-expressing dLNs during EAE. In agreement with the in vitro migration assay, we found that $CD4^+$ T cells expressing CXCR3 and CXCR6 gradually accumulated in the right dLNs of adjuvant-treated mice with EAE, but not in dLNs of EAE-only mice (Figs. 4B and C).

We also measured the distribution of chemokine receptor-expressing $CD4^+$ T cells between the CNS and dLNs of mice with EAE. Notably, over 90% of CNS-infiltrating $CD4^+$ T cells in mice with EAE expressed both CXCR3 and CXCR6 (Fig. 4D). Furthermore, in the inflamed CNS of mice with EAE, $CD4^+$ T cells expressing both CXCR3 and CXCR6 accumulated to significantly greater numbers compared with the CNS of adjuvant-treated mice with EAE (Fig. 4E). The reverse situation was seen in the right dLNs. In adjuvant-EAE mice, $CD4^+$ T cells expressing both CXCR3 and CXCR6 accumulated to significantly

higher numbers compared to those in right dLNs of mice with EAE (Fig. 4E). Thus, in adjuvant-treated mice, high levels of CXCL10 and CXCL16 expression in the right dLNs is followed by the accumulation of $CD4^+$ T cells expressing the cognate receptors CXCR3 and CXCR6 at the same location.

We also measured the distribution of encephalitogenic MOG-specific T cells in the CNS and lymph nodes using an IFN-γ ELISPOT assay. In control mice with EAE, MOG-specific T cells accumulated within the CNS, similar to $CD4^+$ T cells co-expressing CXCR3 and CXCR6 (Figs. 4E versus 4F). However, in adjuvant-treated mice with EAE, MOG-specific T cells accumulated within the right lymph nodes, similar to $CD4^+$ T cells co-expressing CXCR3 and CXCR6 (Figs. 4E versus 4F). There were very few MOG-specific T cells within the non-draining left lymph nodes of adjuvant-EAE mice or EAE mice (Fig. 4F). In adjuvant-treated mice with EAE there were no MOG-specific T cells in the CNS detectable by ELISPOT (Fig. 4F), despite a small population of CNS-infiltrating $CD4^+$ T cells expressing CXCR3 and CXCR6 (Fig. 4D).

Adjuvant pretreatment induces an IFN-γ-dependent inhibition of IL-17 production

In recent years the identification of IL-17 producing Th17 cells and characterization of their importance in driving pathology in EAE (19, 20) has advanced our understanding of the model. The importance of IL-17 producing cells in driving disease and the capacity of IFN-γ to negatively regulate Th17 development (21) provide an explanation for the exacerbated EAE seen in IFN-$\gamma^{-/-}$ mice (22, 23). Next we determined whether MOG-driven IL-17 production was altered by adjuvant-treatment in WT and IFN-$\gamma^{-/-}$ mice. IL-17 production was similarly high in adjuvant-treated IFN-$\gamma^{-/-}$ mice, untreated IFN-$\gamma^{-/-}$ mice, and WT untreated mice with EAE (Fig 5A), consistent with their severe EAE clinical scores (Figs. 1B and 3A). However, WT adjuvant-treated mice with EAE had comparatively low IL-17 levels, which was consistent with the mild EAE scores in this group. These data indicate that adjuvant treatment attenuated IL-17 production during EAE in an IFN-γ-dependent manner. This is in line with earlier studies showing that IFN-γ suppresses development of IL-17 producing cells (24).

In addition to IL-17, the importance of GM-CSF in the pathology of EAE has been highlighted in recent studies(25–27), so we determined the impact of adjuvant-treatment on MOG-induced GM-CSF production. Adjuvant-treatment reduced GM-CSF levels in both wild type and IFN-$\gamma^{-/-}$ mice with EAE (Fig 5B). These results indicate GM-CSF is suppressed by IFN-γ independent means. This provides evidence for IFN-γ-independent protective effects which might account for the delayed onset of EAE in IFN-$\gamma^{-/-}$ mice (Fig. 3A). Additionally, we found no evidence for enhanced production of the regulatory cytokine IL-10 in adjuvant-treated mice with EAE (data not shown), suggesting that adjuvant protection from EAE is due to alterations in the production of pro-inflammatory cytokines and differences in T cell migration rather than enhanced production of IL-10.

4. Discussion

Here we investigated the mechanisms of adjuvant immunotherapy of EAE by killed mycobacteria in CFA. We found that adjuvant treatment prior to EAE induction prevented

autoreactive MOG-specific T cells from accumulating within the CNS. Instead, adjuvant treatment resulted in accumulation of MOG-specific T cells within the dLN of the EAE immunization site. Adjuvant-treatment with CFA did not cause enhanced apoptosis of CNS-infiltrating $CD4^+$ T cells as did live mycobacteria (4). However, we noted that immunization of adjuvant-treated mice to develop EAE led to a coordinated accumulation of large numbers of immature $CD11b^+Gr\text{-}1^+$ myeloid cells, $CD4^+$ T cells, and mycobacteria-specific IFN-γ-producing cells within the dLN at 24 hours. The $CD11b^+$ cells from the dLNs of adjuvant-treated WT, but not adjuvant-treated IFN-$\gamma^{-/-}$ mice, expressed high levels of CXCL10 and CXCL16 transcripts. The dLN cells from adjuvant-treated mice with EAE had an enhanced ability to induce $CD4^+$ T cell migration compared with dLN of EAE-only mice. This chemotactic activity segregated with the $CD11b^+$ myeloid cell population. In vivo, $CD4^+$ T cells co-expressing CXCR3 and CXCR6 and MOG-specific T cells accumulated in the chemokine-expressing dLN of adjuvant-treated mice, but not in the CNS. Furthermore, pro-inflammatory cytokine production in response to MOG was reduced by adjuvant-treatment. Thus, IL-17 production was decreased in adjuvant-treated WT, but not adjuvant-treated IFN-$\gamma^{-/-}$ mice, which reflected the more severe course of disease in adjuvant-treated IFN-$\gamma^{-/-}$ mice with EAE. Also, adjuvant treatment of both WT and IFN-$\gamma^{-/-}$ mice decreased MOG-specific GM-CSF production, indicating additional IFN-γ-independent mechanisms of disease suppression.

The mechanism of CFA-mediated protection of mice from EAE described here shares some features with a mechanism of virus-mediated protection of mice from autoimmune diabetes (28). In the diabetes model, viral infection of mice induced high levels of CXCL10 expression in the lymph nodes relative to the pancreas, indicating a chemokine gradient. Elevated expression of CXCL10 attracted autoreactive T cells from the pancreas into the lymph nodes, thereby sequestering them away from the pancreas. Moreover, the protection of mice from diabetes by viral infection also required IFN-γ. Similarly, we show here that protection from EAE by CFA, as well as expression of CXCL10 and CXCL16 in the lymph nodes both require IFN-γ. Here we extend these studies with the novel finding that immature myeloid cells produce CXCL16 in the same pattern as CXCL10. Moreover, we show that $CD4^+$ T cells expressing the cognate receptors for these chemokines also accumulate in the same lymph nodes where chemokines are expressed.

IFN-beta, which is the most widely used immunotherapy for MS, also induces CXCL10 expression. In patients with MS a transient burst of systemic CXCL10 protein expression was detected at six hours post-IFN-beta injection, with CXCL10 returning to baseline at 24 hours (29). In another report, plasma levels of CXCL10 in MS patients were transiently elevated on day 1, returning to baseline on day 2 (30). A recent study found that among 14 chemokines surveyed by microarray, CXCL10 transcripts and serum levels were strongly upregulated in blood samples at 12 hours post-IFN-beta injection; moreover, blood monocytes were the primary source of CXCL10 (31). These studies suggest a possible mechanism of action for IFN-beta of altering the traffic of CNS cells toward the periphery; however this mechanism remains unproven (32). Such a mechanism may also underlie a promising new therapy for MS. FTY 720 (fingolimod), which modulates sphingosine 1-phosphate receptors, prevents lymphocyte egress from the lymph nodes (33), thereby potentially interfering with lymphocyte recirculation into the CNS. Treatment of MS

patients with fingolimod was associated with reduced rates of relapse (superior to treatment with IFN-beta over 12 months), and reduced CNS lesions detectible by magnetic resonance imaging (34).

As discussed above, studies in both mice and humans have shown that CXCL10 is transiently expressed at high levels and then returns to baseline levels of expression. Yet in this study and in previous reports, T cells expressing the cognate receptor CXCR3 accumulated after even a brief period of elevated CXCL10 production (28, 35, 36). This raises a question of how transient CXCL10 expression promotes the accumulation of $CXCR3^+$ T cells at later time points. However, to the best of our knowledge this question has not been answered. Thus, the temporal regulation of CXCL10 expression and its influence on chemotaxis of $CXCR3^+$ cells remains an unresolved issue that should be addressed in future studies.

A novel finding here is that more than 90% of CNS-infiltrating $CD4^+$ T cells in mice with EAE co-express both CXCR3 and CXCR6. In patients with MS and in mice with EAE, CXCR3 is highly expressed on CNS-infiltrating T cells (37). CXCR6 has been reported to define a population of Th1 and Tc1 cells with extralymphoid tissue homing ability (38). Also, CXCR6 is also a marker of IFN-γ-producing cells in the CNS of MS patients (39). CXCR6 expression was not required for infiltration of T cells into the white matter during EAE, but CXCR6 on T cells was required for injury-induced T cell infiltration into the grey matter of the CNS during EAE(40) . However, the co-expression of CXCR3 and CXCR6 on the majority of CNS infiltrating T cells has not been previously reported in either EAE or in MS.

Here we show a novel function of myeloid derived cells expressing CXCL10 and CXCL16 suggesting that immature myeloid cells can attract T effector cells to the lymph nodes instead of allowing T effector cell migration to the site of tissue antigen and inflammation. There is much clinical interest in how myeloid suppressor cells suppress T cell responses in tumors and infections. Immature myeloid cells can be immunosuppressive during infections, autoimmune responses, and in the tumor microenvironment (41). These cells suppress T cell proliferation by various mechanisms depending on the cytokines present in the microenvironment. For example, immature myeloid cells suppress T cell responses by IL-4 induced production of arginase and by IFN-γ-induced NO and IDO (42–44). We have previously shown that T cell suppression during live mycobacterial infection is mediated by nitric oxide produced by myeloid cells (45, 46). Also we, and others, have shown that myeloid cell-derived NO is required for T cell suppression during EAE (44, 47). Since the role of myeloid-cell-derived iNOS suppressing EAE has already been well studied we did not further investigate the role of iNOS produced by immature myeloid cells in this study. Thus, we cannot rule out a mechanism of NO-mediated T cell suppression in adjuvant-immunotherapy of EAE. Indeed, a previous study demonstrated that iNOS was required for CFA-mediated attenuation of EAE, although myeloid suppressor cells were not defined in the mechanism (48).

The roles of CXCL10 and CXCR3 in CNS inflammation are complex and incompletely understood. CXCL10 protein co-localizing with $CXCR3^+$ cells has been detected within the

CNS during MS and other CNS inflammatory diseases (49). However, conflicting data exist on the impact of neutralization or gene deletion of CXCL10 during EAE—interestingly, the loss of function or neutralization of CXCL10 has been reported to either attenuate or exacerbate EAE in different studies (50–52). Also, the absence of CXCR3 has been reported to either attenuate or exacerbate the severity of EAE (53, 54). Considering these conflicting data, the in vivo neutralization of these molecules to define their protective roles in adjuvant immunotherapy of EAE may not provide unambiguous results. Similarly, as antibody mediated depletion of Gr-1^+ cells in vivo induces resistance to EAE (55) it is not currently possible to isolate the potentially protective role of the $CD11b^+Gr\text{-}1^+$ immature myeloid cells in the draining lymph node of adjuvant pre-treated mice from the pathogenic role of circulating granulocytes.

The above mentioned studies on CXCL10 and CXCR3 suggest these chemokines have biological activities in addition to their chemotactic functions, including effects on T cell priming (56). For example, CXCL10 serves as a dominant chemokine in vitro, capable of attracting T cells away from antigen-bearing immunological synapses (57). It has been suggested that elevated expression of CXCL10 within inflamed tissues might enhance the migration of Th1 cells away from dendritic cells presenting antigens in the lymph nodes. It will be of interest for future studies to understand the biological effects of myeloid-cell-derived CXCL10 on T cell priming within the lymph nodes.

The work presented here adds to a growing body of evidence demonstrating that ongoing Th1 responses are capable of interfering with subsequent Th1 responses in multiple ways. Live infections with virus and mycobacteria promoted IFN-γ-dependent bystander apoptosis of autoreactive T cells (4, 6, 58). Also, exposure to live virus, live mycobacterial infections, and in this study killed mycobacteria, all induced IFN-γ-dependent attraction of autoreactive T cells toward sites of ongoing inflammation rather than toward the antigen-bearing target tissues (58–60) . Furthermore, treatment with CFA reversed diabetes in NOD mice and induced persistently increased numbers of $CD4^+CD25^+Foxp3^+$ regulatory T cells in the pancreatic draining lymph nodes of CFA-treated mice (61).

One implication of our work is that mechanisms of interference by ongoing Th1 responses with subsequent Th1 responses should be considered in designing vaccines to promote Th1 responses to infections and tumors. This concept was recently illustrated by abrogation of anti-tumor protection by using CFA as an adjuvant in a tumor vaccine (62). On the other hand, a better understanding of multiple mechanisms of immune suppression during Th1 responses may allow us to exploit the immune system to halt cell-mediated autoimmune destruction. Finally, as suggested by the hygiene hypothesis, ongoing Th1 responses to ubiquitous saprophytic environmental mycobacteria might counteract the subsequent development of autoimmune diseases (63).

References

1. Gold R. Understanding pathogenesis and therapy of multiple sclerosis via animal models: 70 years of merits and culprits in experimental autoimmune encephalomyelitis research. Brain. 2006; 129:1953–1971. [PubMed: 16632554]

2. Billiau A, Matthys P. Modes of action of Freund's adjuvants in experimental models of autoimmune diseases. J Leukoc Biol. 2001; 70:849–860. [PubMed: 11739546]
3. Kies MW, Alvord EC Jr. [Prevention of allergic encephalomyelitis by prior injection of adjuvants]. Nature. 1958; 182:1106. [PubMed: 13590248]
4. Oconnor R, Wittmer S, Dalton D. Infection-induced apoptosis deletes bystander CD4 T cells: a mechanism for suppression of autoimmunity during BCG infection. Journal of Autoimmunity. 2005; 24:93–100. [PubMed: 15829401]
5. Sewell DL, Reinke EK, Co DO, Hogan LH, Fritz RB, Sandor M, Fabry Z. Infection with Mycobacterium bovis BCG Diverts Traffic of Myelin Oligodendroglial Glycoprotein Autoantigen-Specific T Cells Away from the Central Nervous System and Ameliorates Experimental Autoimmune Encephalomyelitis. Clinical and Vaccine Immunology. 2003; 10:564–572.
6. Qin HY, Chaturvedi P, Singh B. In vivo apoptosis of diabetogenic T cells in NOD mice by IFN-gamma/TNF-alpha. Int Immunol. 2004; 16:1723–1732. [PubMed: 15492021]
7. Chong AS, Shen J, Tao J, Yin D, Kuznetsov A, Hara M, Philipson LH. Reversal of diabetes in non-obese diabetic mice without spleen cell-derived beta cell regeneration. Science. 2006; 311:1774–1775. [PubMed: 16556844]
8. Nishio J, Gaglia JL, Turvey SE, Campbell C, Benoist C, Mathis D. Islet recovery and reversal of murine type 1 diabetes in the absence of any infused spleen cell contribution. Science. 2006; 311:1775–1778. [PubMed: 16556845]
9. Ryu S. Reversal of established autoimmune diabetes by restoration of endogenous beta cell function. Journal of Clinical Investigation. 2001; 108:63–72. [PubMed: 11435458]
10. Suri A, Calderon B, Esparza TJ, Frederick K, Bittner P, Unanue ER. Immunological reversal of autoimmune diabetes without hematopoietic replacement of beta cells. Science. 2006; 311:1778–1780. [PubMed: 16556846]
11. Martins TC, Aguas AP. Mechanisms of Mycobacterium avium-induced resistance against insulin-dependent diabetes mellitus (IDDM) in non-obese diabetic (NOD) mice: role of Fas and Th1 cells. Clin Exp Immunol. 1999; 115:248–254. [PubMed: 9933449]
12. Hempel K, Freitag A, Freitag B, Endres B, Mai B, Liebaldt G. Unresponsiveness to experimental allergic encephalomyelitis in Lewis rats pretreated with complete Freund's adjuvant. Int Arch Allergy Appl Immunol. 1985; 76:193–199. [PubMed: 2579028]
13. Determination of Dosing and Frequency of BCG Administration to Alter T-Lymphocyte Profiles in Type I Diabetics. http://clinicaltrials.gov/ct2/show/NCT00607230
14. Ulaeto D, Lacy PE, Kipnis DM, Kanagawa O, Unanue ER. A T-cell dormant state in the autoimmune process of nonobese diabetic mice treated with complete Freund's adjuvant. Proc Natl Acad Sci U S A. 1992; 89:3927–3931. [PubMed: 1570315]
15. Krakowski ML, Owens T. The central nervous system environment controls effector CD4+ T cell cytokine profile in experimental allergic encephalomyelitis. Eur J Immunol. 1997; 27:2840–2847. [PubMed: 9394808]
16. Matthys P, Vermeire K, Mitera T, Heremans H, Huang S, Schols D, Wolf-Peeters CDe, Billiau A. Enhanced autoimmune arthritis in IFN-gamma receptor-deficient mice is conditioned by mycobacteria in Freund's adjuvant and by increased expansion of Mac-1+ myeloid cells. J Immunol. 1999; 163:3503–3510. [PubMed: 10477624]
17. Wuttge DM. CXCL16/SR-PSOX Is an Interferon-γ-Regulated Chemokine and Scavenger Receptor Expressed in Atherosclerotic Lesions. Arteriosclerosis, Thrombosis, and Vascular Biology. 2004; 24:750–755.
18. Luster AD, Unkeless JC, Ravetch JV. Gamma-interferon transcriptionally regulates an early-response gene containing homology to platelet proteins. Nature. 1985; 315:672–676. [PubMed: 3925348]
19. Langrish CL. IL-23 drives a pathogenic T cell population that induces autoimmune inflammation. Journal of Experimental Medicine. 2005; 201:233–240. [PubMed: 15657292]
20. Hirota K, Martin B, Veldhoen M. Development, regulation and functional capacities of Th17 cells. Semin Immunopathol. 2010; 32:3–16. [PubMed: 20107806]

21. Park H, Li Z, Yang XO, Chang SH, Nurieva R, Wang Y-H, Wang Y, Hood L, Zhu Z, Tian Q, Dong C. A distinct lineage of CD4 T cells regulates tissue inflammation by producing interleukin 17. Nature Immunology. 2005; 6:1133–1141. [PubMed: 16200068]
22. Ferber IA, Brocke S, Taylor-Edwards C, Ridgway W, Dinisco C, Steinman L, Dalton D, Fathman CG. Mice with a disrupted IFN-gamma gene are susceptible to the induction of experimental autoimmune encephalomyelitis (EAE). J Immunol. 1996; 156:5–7. [PubMed: 8598493]
23. Krakowski M, Owens T. Interferon-gamma confers resistance to experimental allergic encephalomyelitis. Eur J Immunol. 1996; 26:1641–1646. [PubMed: 8766573]
24. Harrington LE, Hatton RD, Mangan PR, Turner H, Murphy TL, Murphy KM, Weaver CT. Interleukin 17-producing CD4+ effector T cells develop via a lineage distinct from the T helper type 1 and 2 lineages. Nat Immunol. 2005; 6:1123–1132. [PubMed: 16200070]
25. Codarri L, Gyulveszi G, Tosevski V, Hesske L, Fontana A, Magnenat L, Suter T, Becher B. RORgammat drives production of the cytokine GM-CSF in helper T cells, which is essential for the effector phase of autoimmune neuroinflammation. Nat Immunol. 2011; 12:560–567. [PubMed: 21516112]
26. El-Behi M, Ciric B, Dai H, Yan Y, Cullimore M, Safavi F, Zhang GX, Dittel BN, Rostami A. The encephalitogenicity of T(H)17 cells is dependent on IL-1- and IL-23-induced production of the cytokine GM-CSF. Nat Immunol. 2011; 12:568–575. [PubMed: 21516111]
27. McQualter JL, Darwiche R, Ewing C, Onuki M, Kay TW, Hamilton JA, Reid HH, Bernard CC. Granulocyte macrophage colony-stimulating factor: a new putative therapeutic target in multiple sclerosis. J Exp Med. 2001; 194:873–882. [PubMed: 11581310]
28. Christen U, Benke D, Wolfe T, Rodrigo E, Rhode A, Hughes AC, Oldstone MB, Herrath MGvon. Cure of prediabetic mice by viral infections involves lymphocyte recruitment along an IP-10 gradient. J Clin Invest. 2004; 113:74–84. [PubMed: 14702111]
29. Buttmann M, Merzyn C, Rieckmann P. Interferon-beta induces transient systemic IP-10/CXCL10 chemokine release in patients with multiple sclerosis. J Neuroimmunol. 2004; 156:195–203. [PubMed: 15465611]
30. Krakauer M, Sorensen PS, Khademi M, Olsson T, Sellebjerg F. Dynamic T-lymphocyte chemokine receptor expression induced by interferon-beta therapy in multiple sclerosis. Scand J Immunol. 2006; 64:155–163. [PubMed: 16867161]
31. Cepok S, Schreiber H, Hoffmann S, Zhou D, Neuhaus O, Geldern Gvon, Hochgesand S, Nessler S, Rothhammer V, Lang M, Hartung HP, Hemmer B. Enhancement of chemokine expression by interferon beta therapy in patients with multiple sclerosis. Arch Neurol. 2009; 66:1216–1223. [PubMed: 19667211]
32. Stuve O, Ransohoff RM. Immunotherapy for multiple sclerosis: the curious case of interferon beta. Arch Neurol. 2009; 66:1193–1194. [PubMed: 19822773]
33. Schwab SR, Cyster JG. Finding a way out: lymphocyte egress from lymphoid organs. Nat Immunol. 2007; 8:1295–1301. [PubMed: 18026082]
34. Cohen JA, Barkhof F, Comi G, Hartung HP, Khatri BO, Montalban X, Pelletier J, Capra R, Gallo P, Izquierdo G, Tiel-Wilck K, Vera Ade, Jin J, Stites T, Wu S, Aradhye S, Kappos L. Oral fingolimod or intramuscular interferon for relapsing multiple sclerosis. N Engl J Med. 2010; 362:402–415. [PubMed: 20089954]
35. Christen U, McGavern DB, Luster AD, Herrath MGvon, Oldstone MB. Among CXCR3 chemokines, IFN-gamma-inducible protein of 10 kDa (CXC chemokine ligand (CXCL) 10) but not monokine induced by IFN-gamma (CXCL9) imprints a pattern for the subsequent development of autoimmune disease. J Immunol. 2003; 171:6838–6845. [PubMed: 14662890]
36. Medoff BD, Sauty A, Tager AM, Maclean JA, Smith RN, Mathew A, Dufour JH, Luster AD. IFN-gamma-inducible protein 10 (CXCL10) contributes to airway hyperreactivity and airway inflammation in a mouse model of asthma. J Immunol. 2002; 168:5278–5286. [PubMed: 11994485]
37. Balashov KE, Rottman JB, Weiner HL, Hancock WW. CCR5(+) and CXCR3(+) T cells are increased in multiple sclerosis and their ligands MIP-1alpha and IP-10 are expressed in demyelinating brain lesions. Proc Natl Acad Sci U S A. 1999; 96:6873–6878. [PubMed: 10359806]

38. Kim CH, Kunkel EJ, Boisvert J, Johnston B, Campbell JJ, Genovese MC, Greenberg HB, Butcher EC. Bonzo/CXCR6 expression defines type 1-polarized T-cell subsets with extralymphoid tissue homing potential. J Clin Invest. 2001; 107:595–601. [PubMed: 11238560]
39. Calabresi PA, Yun SH, Allie R, Whartenby KA. Chemokine receptor expression on MBP-reactive T cells: CXCR6 is a marker of IFNgamma-producing effector cells. J Neuroimmunol. 2002; 127:96–105. [PubMed: 12044980]
40. Kim JV, Jiang N, Tadokoro CE, Liu L, Ransohoff RM, Lafaille JJ, Dustin ML. Two-photon laser scanning microscopy imaging of intact spinal cord and cerebral cortex reveals requirement for CXCR6 and neuroinflammation in immune cell infiltration of cortical injury sites. J Immunol Methods. 352:89–100. [PubMed: 19800886]
41. Gabrilovich DI, Nagaraj S. Myeloid-derived suppressor cells as regulators of the immune system. Nat Rev Immunol. 2009; 9:162–174. [PubMed: 19197294]
42. Bronte V, Serafini P, Santo CDe, Marigo I, Tosello V, Mazzoni A, Segal DM, Staib C, Lowel M, Sutter G, Colombo MP, Zanovello P. IL-4-induced arginase 1 suppresses alloreactive T cells in tumor-bearing mice. J Immunol. 2003; 170:270–278. [PubMed: 12496409]
43. Munn DH, Mellor AL. IDO and tolerance to tumors. Trends Mol Med. 2004; 10:15–18. [PubMed: 14720581]
44. Zhu B, Bando Y, Xiao S, Yang K, Anderson AC, Kuchroo VK, Khoury SJ. CD11b+Ly-6C(hi) suppressive monocytes in experimental autoimmune encephalomyelitis. J Immunol. 2007; 179:5228–5237. [PubMed: 17911608]
45. Li X, McKinstry KK, Swain SL, Dalton DK. IFN-gamma acts directly on activated CD4+ T cells during mycobacterial infection to promote apoptosis by inducing components of the intracellular apoptosis machinery and by inducing extracellular proapoptotic signals. J Immunol. 2007; 179:939–949. [PubMed: 17617585]
46. Dalton DK, Haynes L, Chu CQ, Swain SL, Wittmer S. Interferon gamma eliminates responding CD4 T cells during mycobacterial infection by inducing apoptosis of activated CD4 T cells. J Exp Med. 2000; 192:117–122. [PubMed: 10880532]
47. Dalton D, Wittmer S. Nitric-oxide-dependent and independent mechanisms of protection from CNS inflammation during Th1-mediated autoimmunity: evidence from EAE in iNOS KO mice. Journal of Neuroimmunology. 2005; 160:110–121. [PubMed: 15710464]
48. Kahn DA, Archer DC, Gold DP, Kelly CJ. Adjuvant immunotherapy is dependent on inducible nitric oxide synthase. J Exp Med. 2001; 193:1261–1268. [PubMed: 11390433]
49. Müller M, Carter S, Hofer MJ, Campbell IL. Review: The chemokine receptor CXCR3 and its ligands CXCL9, CXCL10 and CXCL11 in neuroimmunity - a tale of conflict and conundrum. Neuropathology and Applied Neurobiology. 2010; 36:368–387. [PubMed: 20487305]
50. Fife BT, Kennedy KJ, Paniagua MC, Lukacs NW, Kunkel SL, Luster AD, Karpus WJ. CXCL10 (IFN-gamma-inducible protein-10) control of encephalitogenic CD4+ T cell accumulation in the central nervous system during experimental autoimmune encephalomyelitis. J Immunol. 2001; 166:7617–7624. [PubMed: 11390519]
51. Klein RS, Izikson L, Means T, Gibson HD, Lin E, Sobel RA, Weiner HL, Luster AD. IFN-inducible protein 10/CXC chemokine ligand 10-independent induction of experimental autoimmune encephalomyelitis. J Immunol. 2004; 172:550–559. [PubMed: 14688366]
52. Narumi S, Kaburaki T, Yoneyama H, Iwamura H, Kobayashi Y, Matsushima K. Neutralization of IFN-inducible protein 10/CXCL10 exacerbates experimental autoimmune encephalomyelitis. Eur J Immunol. 2002; 32:1784–1791. [PubMed: 12115662]
53. Liu L, Huang D, Matsui M, He TT, Hu T, Demartino J, Lu B, Gerard C, Ransohoff RM. Severe disease, unaltered leukocyte migration, and reduced IFN-gamma production in CXCR3−/− mice with experimental autoimmune encephalomyelitis. J Immunol. 2006; 176:4399–4409. [PubMed: 16547278]
54. Muller M, Carter SL, Hofer MJ, Manders P, Getts DR, Getts MT, Dreykluft A, Lu B, Gerard C, King NJ, Campbell IL. CXCR3 signaling reduces the severity of experimental autoimmune encephalomyelitis by controlling the parenchymal distribution of effector and regulatory T cells in the central nervous system. J Immunol. 2007; 179:2774–2786. [PubMed: 17709491]

55. McColl SR, Staykova MA, Wozniak A, Fordham S, Bruce J, Willenborg DO. Treatment with anti-granulocyte antibodies inhibits the effector phase of experimental autoimmune encephalomyelitis. J Immunol. 1998; 161:6421–6426. [PubMed: 9834134]
56. Groom JR, Luster AD. CXCR3 in T cell function. Exp Cell Res. 2011; 317:620–631. [PubMed: 21376175]
57. Bromley SK, Peterson DA, Gunn MD, Dustin ML. Cutting edge: hierarchy of chemokine receptor and TCR signals regulating T cell migration and proliferation. J Immunol. 2000; 165:15–19. [PubMed: 10861029]
58. Christen U. Cure of prediabetic mice by viral infections involves lymphocyte recruitment along an IP-10 gradient. Journal of Clinical Investigation. 2004; 113:74–84. [PubMed: 14702111]
59. Sewell DL, Reinke EK, Co DO, Hogan LH, Fritz RB, Sandor M, Fabry Z. Infection with Mycobacterium bovis BCG diverts traffic of myelin oligodendroglial glycoprotein autoantigen-specific T cells away from the central nervous system and ameliorates experimental autoimmune encephalomyelitis. Clin Diagn Lab Immunol. 2003; 10:564–572. [PubMed: 12853387]
60. Lee J, Sandor M, Heninger E, Fabry Z. Mycobacteria-induced suppression of autoimmunity in the central nervous system. J Neuroimmune Pharmacol. 2010; 5:210–219. [PubMed: 20333556]
61. Tian B, Hao J, Zhang Y, Tian L, Yi H, O'Brien TD, Sutherland DER, Hering BJ, Guo Z. Upregulating CD4+CD25+FOXP3+ Regulatory T Cells in Pancreatic Lymph Nodes in Diabetic NOD Mice by Adjuvant Immunotherapy. Transplantation. 2009; 87:198–206. [PubMed: 19155973]
62. Wang Z, Jiang J, Li Z, Zhang J, Wang H, Qin Z. A myeloid cell population induced by Freund adjuvant suppresses T-cell-mediated antitumor immunity. J Immunother. 2010; 33:167–177. [PubMed: 20145547]
63. Rook GA. The hygiene hypothesis and the increasing prevalence of chronic inflammatory disorders. Trans R Soc Trop Med Hyg. 2007; 101:1072–1074. [PubMed: 17619029]

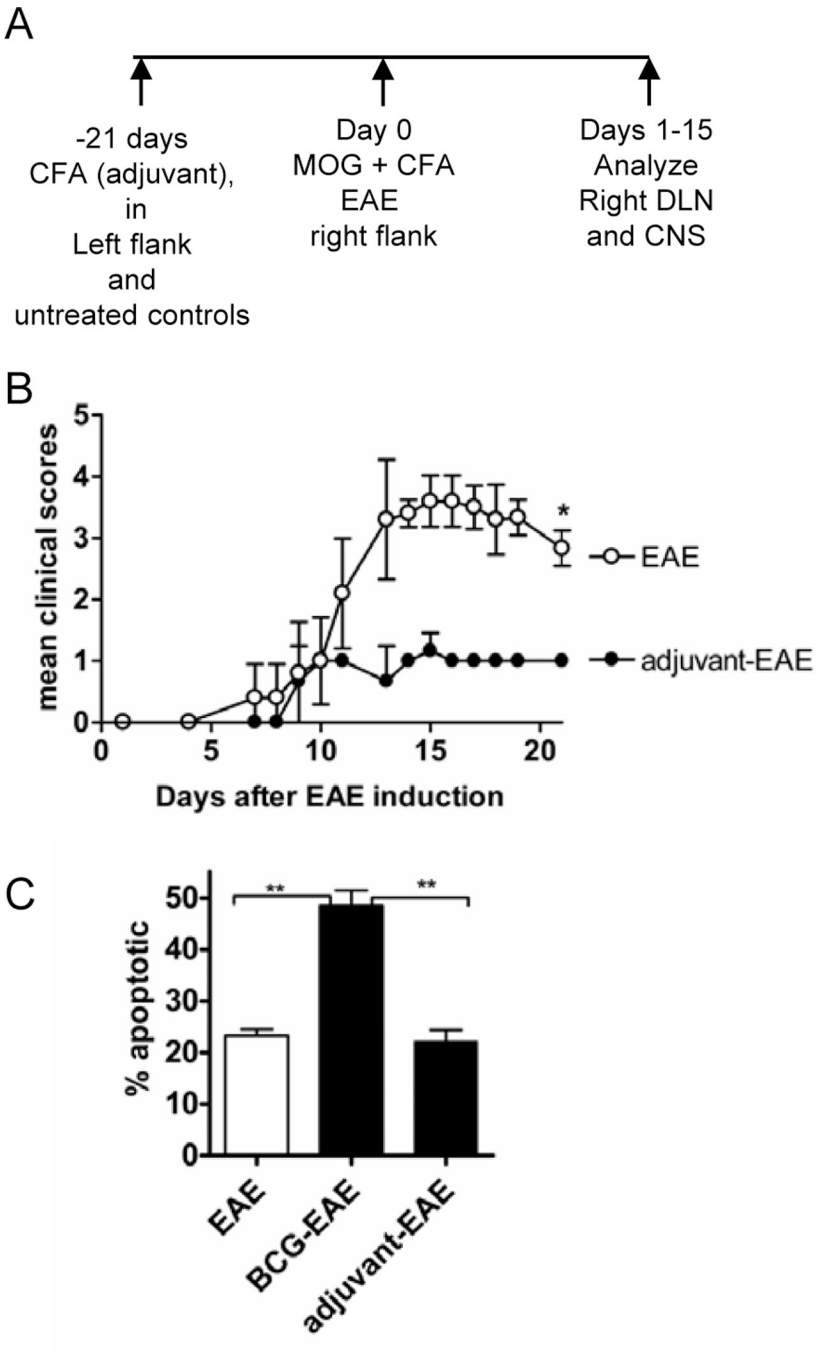

Figure 1. Adjuvant-treatment with CFA attenuated clinical EAE, but did not increase apoptosis of CNS-infiltrating T cells

(A) The experimental design is shown. Adjuvant-EAE mice were treated with CFA on the left flank or mice were left untreated for EAE-only. On day 21 after CFA treatment, EAE was induced in mice with ($MOG_{35–55}$) emulsified in CFA. (B) Clinical course of EAE in naïve and adjuvant-treated WT mice. (*P=0.02 Mann-Whitney Test) (C) The percentage of apoptotic CNS-infiltrating $CD4^+$ T cells was measured by Annexin-V/PI staining at the end

of the experiment (day 21). Shown is the mean and SD of 4 mice per group (**P≤0.002 by T-test); two independent experiments were done.

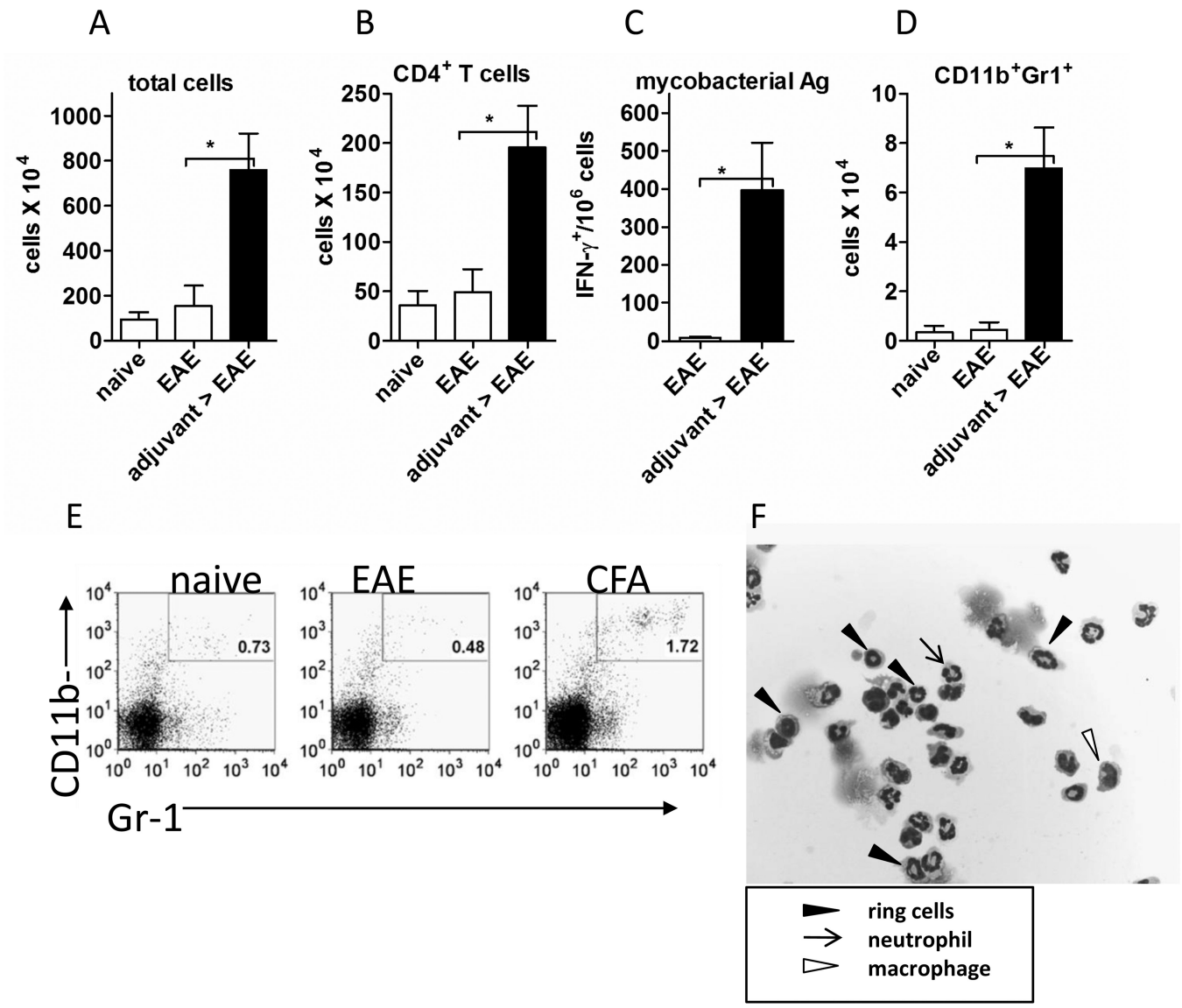

Figure 2. Adjuvant-treated mice responded to EAE induction by rapidly mobilizing immature myeloid cells and CFA-specific IFN-γ^+ T cells to the right lymph nodes

EAE was induced in adjuvant-treated and control mice. Analysis of the draining lymph nodes was done 24 hours later. (A) Total number of cells in dLNs. (B) Total numbers of $CD4^+$ T cells in the right dLNs. (C) Total numbers of $CD11b^+Gr\text{-}1^+$ cells in right draining lymph nodes (D) Frequency of right dLN cells producing IFN-γ in response to killed *Mycobacterium tuberculosis* as measured by ELISPOT. (E) Representative FACS plots of right draining lymph nodes showing the $CD11b^+Gr\text{-}1^+$ population in naïve, EAE, and adjuvant-EAE mice. Percentage of live cells expressing both CD11b and Gr-1 are shown in each plot. (F) Morphology of the $CD11b^+Gr\text{-}1^+$ cells from the right draining lymph nodes of adjuvant- EAE mice. The cells were sorted to purity by FACS, part of the cell suspension was prepared by cytospin and then stained with hematoxylin & eosin. Boxed legend indicates cell subsets. In A–C the total number of cells was determined by hemacytometer counting. The cells were analyzed using flow cytometry to determine the percentage of live

cells expressing indicated markers. In A–D the mean and SEM of 3 mice per group is shown; representative of at least two experiments.*P ≤0.03 by the unpaired T-test.

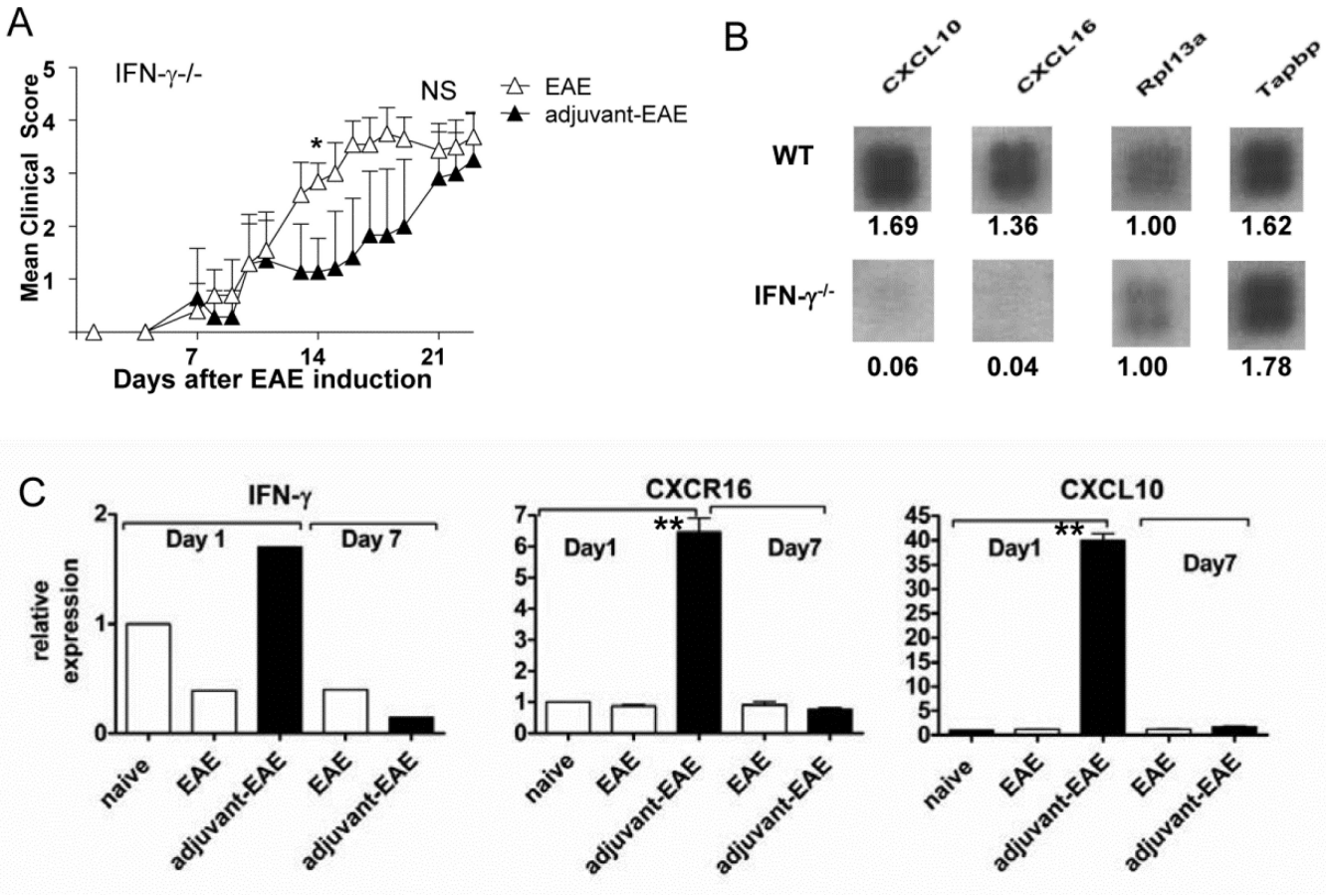

Figure 3. IFN-$\gamma^{-/-}$ is required both for adjuvant-mediated attenuation of EAE and for CXCL10 and CXCL16 chemokine expression by immature myeloid cells in the lymph nodes

(A) Clinical EAE scores are shown for untreated and adjuvant-treated IFN-$\gamma^{-/-}$ mice. Shown is the mean and SD of 10 mice per group (pooled data from two independent experiments). *d14, scores are significantly different (by Mann-Whitney Test). On day 21 there was no significant difference in EAE scores between groups (NS). (B) Images of CXCL10 and CXCL16 from chemokine microarrays using RNA from sorted dLN CD11b^{+} cells from adjuvant-EAE mice. Numbers below each cloverleaf spot represent the relative density of the signal (normalized to density of Rpl3a, which was equal in WT and IFN-$\gamma^{-/-}$ mice). (C) Validation of microarray data by RT PCR analysis. The kinetics of IFN-γ, CXCL10, and CXCL16 mRNA in whole dLN cells from naïve, WT EAE and WT adjuvant-EAE mice was measured by RT PCR. Graphs show relative expression (to naïve) of IFN-γ, CXCL10, and CXCL16 in right draining lymph nodes of indicated mice on days 1 and 7 after EAE was induced. Results shown are the mean and SEM of 4- 6 mice per group, measured in two independent experiments. (**P<0.0001 unpaired T-test).

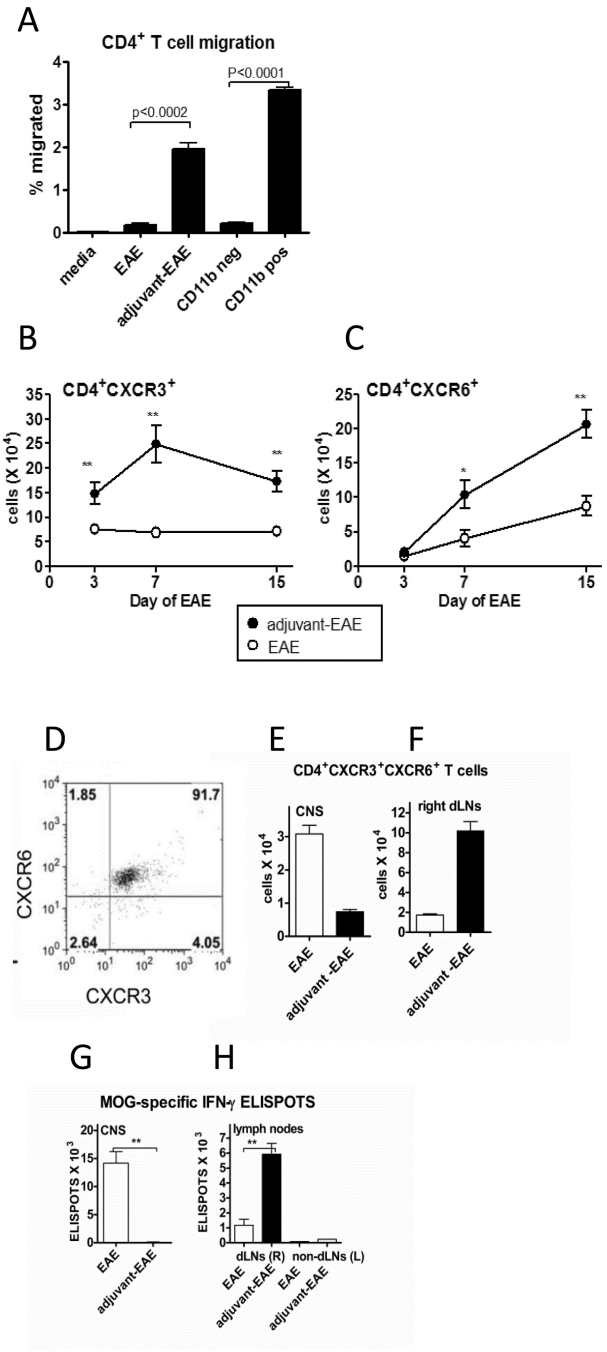

Figure 4. MOG-specific T cells as well as CD4$^+$ T cells expressing both CXCR3 and CXCR6 accumulated within the right draining lymph nodes of adjuvant-treated mice with EAE instead of accumulating within the CNS

(A) Results of an in vitro chemotaxis assay. The percentage of input CD4$^+$ T cells which migrated towards the indicated cell populations in the lower wells of a transwell plate. CD4$^+$ T cells were isolated from adjuvant-EAE dLN (day 1 EAE) and added to top wells (2×10^5). Lower well populations are indicated on the X-axis. Lower wells contained 2×10^6 cells derived from whole dLN on day 1 of EAE using EAE and adjuvant-EAE mice. CD11b^{neg} cells are whole dLN cells from adjuvant-EAE mice depleted of CD11b cells by MACS.

$CD11b^{pos}$ are MACS-purified cells from dLN of adjuvant-EAE mice on day 1 of EAE. P values above bar graphs are from a one-way ANOVA. Each point is the mean and SEM of 3 mice per group; representative of two independent experiments. (B) Total numbers of $CD4^+CXCR3^+$ T cells and (C) $CD4^+CXCR6^+$ T cells in lymph nodes from adjuvant-EAE and EAE mice on days 3, 7, and 15 post-EAE induction. The mean and SEM are shown for 6 mice per group, **$p \leq 0.002$ by unpaired T-test (*$P \leq 0.03$). (D) Representative dot plot (of n=6 mice) showing co-expression of CXCR3 and CXCR6 on CNS-infiltrating $CD4^+$ T cells of mice with EAE (day 15). Numbers in quadrants indicate percentage of cells in each subset. Gated on live $CD4^+$ T cells. (E) Absolute numbers of $CD4^+CXCR3^+CXCR6^+$ T cells in CNS of indicated mice on day 15 of EAE. (mean and SEM of 6 mice per point). (F) Absolute numbers of $CD4^+CXCR3^+CXCR6^+$ T cells in right dLNs of indicated mice on day 15 of EAE, (mean and SEM of 6 mice per point). (G) Total number of MOG-specific T cells in the CNS on day 15 of EAE was determined by an IFN-γ ELISPOT assay, (mean and SEM of 6 mice per point). (H) Total number of MOG-specific T cells in right (R) and left (L) dLNs on day 15 of EAE was determined by an IFN-γ ELISPOT assay, (mean and SEM of 6 mice per point), **$P \leq 0.0022$ by Mann-Whitney test, except where otherwise noted.).

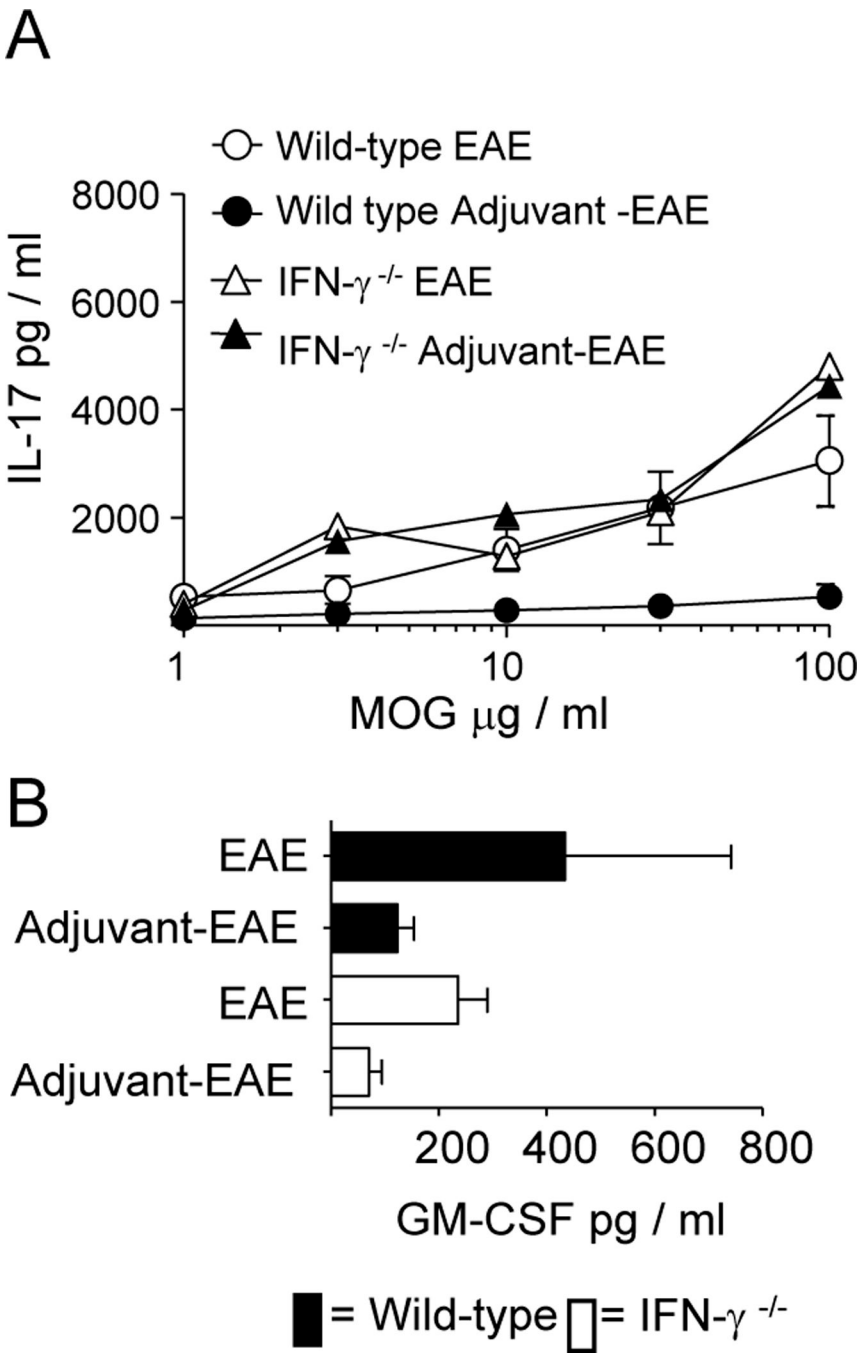

Figure 5. Adjuvant treatment suppresses MOG-specific IL-17 production in wild type but not IFN-$\gamma^{-/-}$ mice

Wild type and IFN-$\gamma^{-/-}$ mice were adjuvant-treated or left untreated as previously described (n=6 per group). 21 days later mice were immunized with MOG/CFA on the right flank. Mice were sacrificed 7 days post MOG/CFA-immunization. A) IL-17-production by splenocytes in response to MOG. B) GM-CSF-production by splenocytes in response to 30 μg / ml MOG.